energies

MDPI

Article

Constraint Satisfaction in Current Control of a Five-Phase Drive with Locally Tuned Predictive Controllers

Agnieszka Kowal G. [1], Manuel R. Arahal [1,*], Cristina Martin [2] and Federico Barrero [2]

[1] Systems Engineering and Automation Department, University of Seville, 41092 Seville, Spain
[2] Electronic Engineering Department, University of Seville, 41092 Seville, Spain
* Correspondence: arahal@us.es; Tel.: +34-954-48-73-43

Received: 9 May 2019; Accepted: 10 July 2019; Published: 16 July 2019

Abstract: The problem of control of stator currents in multi-phase induction machines has recently been tackled by direct digital model predictive control. Although these predictive controllers can directly incorporate constraints, most reported applications for stator current control of drives do no use this possibility, being the usual practice tuning the controller to achieve the particular compromise solution. The proposal of this paper is to change the form of the tuning problem of predictive controllers so that constraints are explicitly taken into account. This is done by considering multiple controllers that are locally optimal. To illustrate the method, a five-phase drive is considered and the problem of minimizing $x - y$ losses while simultaneously maintaining the switching frequency and current tracking error below some limits is tackled. The experiments showed that the constraint feasibility problem has, in general, no solution for standard predictive control, whereas the proposed scheme provides good tracking performance without violating constraints in switching frequency and at the same time reducing parasitic currents of $x - y$ subspaces.

Keywords: constraints satisfaction; cost functions; local controllers; predictive current control; multi-phase drives

1. Introduction

This papers deals with stator current control of Induction Machines (IM) with more than three phases. It is well known that Model Based Predictive Control (MBPC) can be applied for this task in a configuration where the controller directly commands the inverter without modulation techniques [1]. This control scheme is a particular case of the more general Finite State Model Predictive Control and is often referred to as Predictive Current Control (PCC) [2–4]. Recently, PCC has received increasing attention as an interesting choice for multi-phase and/or multi-level systems.

One of the key aspects of MBPC is the possibility of handling constraints directly [5] and, thus, the PCC could benefit from the constraint-handling capability of MBPC, however in most reported cases this possibility is not used. Instead, the usual practice is tuning the controller to achieve the particular compromise solution [6]. Thus, the selection of the controller parameters is made based on the expected behavior of the IM considering some operating regions. It must be recalled that in PCC the instantaneous minimization of the cost function imprints in the IM certain current waveforms that in turn produce a a certain global behavior. It is often found that such behavior contains conflicting criteria, thus PCC design should meet the underlying trade-offs [7]. According to this, PCC tuning should translate objectives such as commutations, tracking quality, etc. to control parameters, which is not an easy task. Regarding this, several methods have been proposed to tune the MBPC for drives in a more or less automatic fashion (see [8,9] for a review of methods), but the constraint satisfaction is not considered.

The proposal of this paper is to change the form of the tuning problem of MBPC so that constraints are explicitly taken into account. It is shown that this can be done by considering multiple controllers that are locally optimal in a way similar to the proposal in [10], where, by solving the optimization problem differently for each operating region, a better global behavior can be attained.

To illustrate the method, in this paper a five-phase drive is considered. The higher number of phases (compared to the standard three-phase case) provides further room for optimization, more tuning possibilities and complex trade-offs between the different figures of merit. For this application, the problem of minimizing $x - y$ losses while simultaneously maintaining the switching frequency and current tracking error below some limits is considered. For other applications, other figures of merit could be used, for instance harmonic distortion in Uninterrupted Power Systems [11], current ripple in permanent magnet motors [12], speed in wind turbines [13] and others.

The chosen example problem is relevant as the five-phase machine is of interest [14] and the proposed minimization would reduce losses without compromising dynamic performance and ensuring a switching frequency adequate for the available hardware. Please notice that the strategy is applicable to other types of systems, being the five-phase IM a particularly interesting and demanding case study that requires dealing with the extra number of phases. Application to other multi-phase systems such as the six-phase IM is straightforward thanks to the vector space decomposition technique [15].

In the next section, the basic aspects of PCC are reviewed, introducing the figures of merit that are considered in the proposal for MBPC tuning. The concept of constraint handling via local controllers is presented in Section 3 including the partition of operating space and the local tuning method. The resulting controller is assessed in Section 4, paying special attention to the constraint feasibility problem for the whole operating space. From these results, some conclusions are derived in Section 5.

2. PCC for Five-Phase IM

A brief introduction to PCC is now given to ease the presentation of the proposed variation. Although the description is given for the specific case of a five-phase IM, only minor adjustment are needed for a different number of phases thanks to the state-space representation.

According to the block diagram of PCC shown in Figure 1, the IM is driven by a Voltage Source Inverter (VSI) that provides a certain set of phase voltages v that are derived from the control signal u and the VSI topology. This produces stator phase currents i that follow a vector of sinusoidal reference trajectories i^*. The PCC uses a model of the IM and VSI to predict the evolution of the stator currents associated to each possible VSI state. The controller optimizes, by exhaustive search, the control move for discrete time $k + 1$, which is held for a sampling period. The procedure is then repeated according to the receding horizon rule typical of predictive controllers.

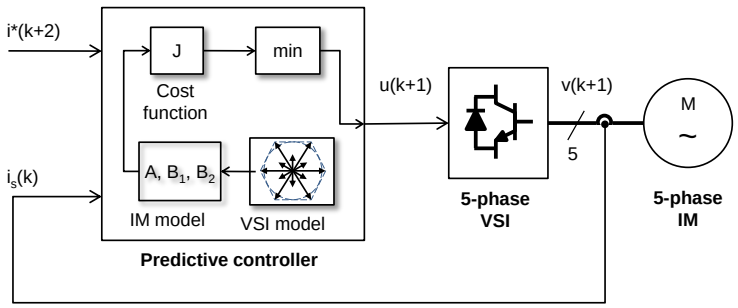

Figure 1. Diagram of predictive stator current control of a five-phase IM fed by a VSI.

In the case of multi-phase IM with n phases, the vector space decomposition technique provides the decomposition of the n-phase space into one $\alpha - \beta$ plane, which is responsible for energy conversion and some other planes: $(x - y)^1$ to $(x - y)^{(n-4)/2}$ that are related to copper losses. The voltages

produced by the VSI are mapped to these subspaces to form a row vector $v_{\alpha\beta xys} = (v_{\alpha s}, v_{\beta s}, v_{xs}, v_{ys})$ by means of

$$v_{\alpha\beta xys} = V_{dc} u T M \tag{1}$$

where V_{dc} is the DC link voltage, T is a connectivity matrix that takes into account how the VSI gating signals are distributed and M is a coordinate transformation matrix accounting for the spatial distribution of machine windings. In the case of a three-phase IM, there is no $x-y$ subspace. In the case of the five-phase IM, only one auxiliary plane exists. For other multi-phase systems, the extra number of subspaces are easily treated using the state-space representation. From this decomposition, and using time-discretization, the following predictive model is obtained

$$\hat{i}(k+2|k) = Ai(k) + B_1 u(k) + B_2 u(k+1) + G(k) \tag{2}$$

where matrices A, B_1 and B_2 are related to the IM electrical parameters and to the VSI connections. In addition, matrix A is not constant but dependent on the electrical frequency $A(\omega_r)$ [16]. A state space vector can be considered including stator currents in the principal and secondary planes such as $i = \left(i_\alpha, i_\beta, i_x, i_y\right)^\top$. This vector can be obtained from sensors transforming the phase stator currents i_s into $\alpha-\beta$ and $x-y$ subspaces by means of the inverse transformation to that given in Equation (1). Vector G accounts for the dynamics due to rotor currents that are usually not measured. It constitutes a term that must be estimated at each k [17,18].

In Equation (2), the control signal u is a vector of gating signals of the VSI $u = (K_1, K_2, \ldots, K_5)^\top$, where $K_i \in \{0,\ 1\}$ for $i = 1, \ldots, 5$. Each of the five phases can be connected through the VSI to the positive ($K_i = 1$) or negative ($K_i = 0$) borne of the DC-link. In this way, the VSI can produce $\tau = 2^5$ different phase voltages. Due to redundancy, only 31 different voltages are actually produced [19].

In most applications of PCC, for discrete time k, a value of the control signal is selected for the next sampling period $u(k+1)$ by minimizing some objective function J. This objective function can be the sum of a number of quadratic terms penalizing control error, control effort, etc. [5]. The simplest objective function includes the square of the predicted control error $\hat{e} = (i^* - \hat{i})$. In the case of drives, sometimes a penalization of VSI commutations is included. This is achieved by computing the number of switch changes SC produced at the VSI when the previous state $u(k)$ is changed to any other $u(k+1)$ as $SC(k) = \sum_{i=1}^{5} |u_i(k+1) - u_i(k)|$, and the switching frequency f_{sw} is$f_{sw} = \sum_{k=k_1}^{k_2} SC(k)/(T_s(k_2 - k_1 + 1))$, where T_s is the sampling time. Please notice that the switching frequency in PCC is not constant. This drawback is a consequence of the direct digital control approach. Although this can be alleviated by using some techniques, the benefits from the elimination of the modulation stage are deemed more important in most cases. Nevertheless, the average switching frequency should not exceed some limits imposed by the VSI hardware. In addition, to limit commutation losses high values of f_{sw} should be avoided. Finally, the $x-y$ currents do not produce torque and are related to losses, thus it is customary to set their reference to zero. Taking these considerations into account, the cost function takes the form

$$J = \|\hat{e}_{\alpha\beta}\|^2 + \lambda_{xy}\|\hat{e}_{xy}\|^2 + \lambda_{sc} SC \tag{3}$$

where $\|.\|$ is the vector modulus operation. It can be seen that two parameters (λ_{xy} and λ_{sc}) are needed to take into account the different scales of the variables included in the cost function. In addition, these parameters are typically used to set the relative importance of the three objectives. In a traditional PCC setup, these factors are computed off-line as a compromise between conflicting criteria and considering (in the best of cases) the whole range of operation of the system, as in [6]. The computed values are then used on-line. This way of proceeding seems subject to potential improvement as it is realized that, for different regions of operation, the terms present in Equation (3) take different relative values. For instance, for low speed and load, the IM shows larger harmonic distortion and lower switching frequency, whereas, for medium speed and load, the situation is the opposite [7].

3. Constraint Handling with Local Controllers

The problem associated with constraints in PCC is that the minimization of Equation (3) does not guarantee a certain quality of tracking or a certain commutation rate. This is because the minimization of Equation (3) takes place at each sampling time without regard the choices made in previous periods. A possible path to overcome this would be determining a set of controller parameters (λ_{xy} and λ_{sc}) to attain the desired behavior. The following optimization problem can then be used

$$\begin{aligned} \min_{\theta} \quad & E_{xy} \\ \text{s.t.} \quad & E_{\alpha\beta} < U_{\alpha\beta} \\ & \max f_{sw} < U_{sw} \end{aligned} \tag{4}$$

where $\theta = (\lambda_{xy}, \lambda_{SC})$ is the generic element of the search space, $E_{\alpha\beta}$ is the root mean squared error obtained for tracking of $\alpha - \beta$ stator currents, E_{xy} is the root mean squared error obtained for regulation of $x - y$ stator currents, and $\max f_{sw}$ is the highest recorded value for the switching frequency f_{sw}.

With this design procedure a minimization of $x - y$ related losses is sought ensuring at the same time that the tracking error is below some limit $U_{\alpha\beta}$ and that the VSI would not exceed a limit U_{sw} set on the switching frequency f_{sw}. Unfortunately, this problem, in general, not solvable for all operating regimes because no feasible solutions exist [7]. It is shown that using locally tuned controllers it is possible to attain a solution for each operating regime.

3.1. Local Controllers

The concept of Local Controllers is similar to other well known methods such as the Self Tuning Regulator [20] and Gain Scheduling [21]. The original ideas of dividing a non-linear design problem into linear sub-problems have spurred many variations including the strategy known as Local Controller Networks [22] where a set of controllers is considered instead of just a fixed one. At any given moment, only one controller from the set is allowed to act. The decision of which controller should be used is based on a handful of variables related to the current state of the system. This scheme can work provided that for each state an adequate/optimal controller can be uniquely determined. When the controllers in the set share the same structure and differ only in some parameters, the problem of controller selection becomes one of parameter selection. These parameters can be computed to be optimal in a, probably small, region of the system's operating space. In this sense, the tuning (parameter selection) takes place locally, giving rise to the denomination of Local Tuning Parameters.

3.2. Partition of Operating Space

The selection of regions where local controllers are defined is not a trivial task in a general case. For the particular case of PCC of an IM drive, expert knowledge suggests using speed ω and load T as scheduling variables. Considering the range of variation of these variables for a particular IM, the operating space can be defined as $\Phi = [0,\ \overline{\omega}] \times [0,\ \overline{T}]$ where the over line indicates maximum value.

The partition of Φ can be done in different ways, being the simpler a set of rectangular cells in the form $[h\Delta\omega,\ (h+1)\Delta\omega] \times [j\Delta T,\ (j+1)\Delta T]$ obtained considering some increments $\Delta\omega$ and ΔT. For smaller increments, the obtained partition is finer enabling a higher possibility of obtaining an adequate scheduling.

Once the partition has been made, the MBPC λ parameters can be found via simulation for each region as will be shown next.

3.3. Local Tuning

For each cell $\phi_{hj} \in \Phi$ defined as $\phi_{hj} = [h\Delta\omega,\ (h+1)\Delta\omega] \times [j\Delta T,\ (j+1)\Delta T]$ the controller parameters are selected as the solutions of Equation (4). The limits can be the same for all operating points or follow some other rule. This is important as the minimization problem of Equation (4) can

have no solutions if the limits are too tight. To solve Equation (4), an optimization algorithm linked to a simulation of the drive must be used. The five-phase IM, the VSI and the PCC are simulated using a Runge–Kutta method including the controller as a discrete-time part considering its computing times. The IM parameters are those of the real IM in the experimental setup that are used later for confirmation. A sampling time of $80 \cdot 10^{-6}$ s has been used for the controller. This sampling time is enough for most modern digital signal processors to run the PCC code. Following the idea of locally tuned controllers, the simulation considers operation around each of the considered center of the partition of the operating space. The magnitude of changes must ensure that the operation remains inside the considered cell. The order of events have been found not to alter the results provided that the simulations contain enough data samples (i.e., they are not too short).

4. Results

The constraint satisfaction capability of the proposed controller is assessed using computer simulations and laboratory tests in the experimental setup shown in Figure 2. The equipment used includes a 30-slot symmetrical five-phase induction machine with distributed windings and three pole pairs. The IM is electrically supplied by means of two three-phase two-level inverters (Semikron SKS22F modules), one of which has an unused phase. A DC-link voltage of 300 (V) is applied to both modules. The predictive controller runs on a TMS320F28335 digital signal processor embedded in a MSK28335 Technosoft board with the appropriate digital and analog input/output connections. The rotor mechanical speed is measured using a GHM510296R/2500 digital rotatory encoder. The experimental setup also includes an independently controlled DC machine that is used to produce load torque in the shaft of the IM machine. In this way, different loading conditions can be tested. The electrical parameters (inductances and resistances) have been identified through experimentation, as explained in [23], and are shown in Table 1.

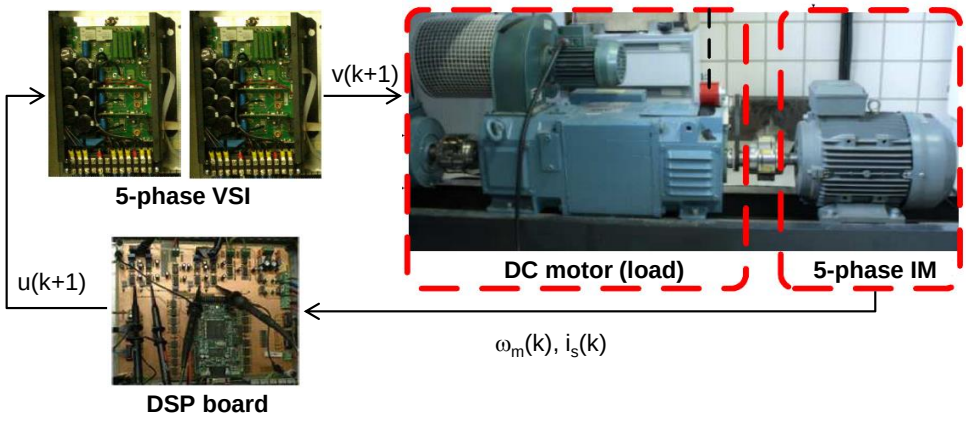

Figure 2. Photographs of the various elements of the experimental setup.

Table 1. Estimated parameters of the IM.

Parameter		Value	Parameter		Value
Stator resistance	R_s (Ω)	19.45	Rotor resistance	R_r (Ω)	6.77
Stator leakage inductance	L_{ls} (mH)	100.7	Rotor leakage inductance	L_{lr} (mH)	38.6
Mutual inductance	L_m (mH)	656.5	Nominal current	I_n (A)	2.5
Mechanical nominal speed	ω_n (rpm)	1000	Nominal torque	T_n (N·m)	4.7

In Figure 3(left), the feasible region for $U_{\alpha\beta} = 0.035$ (A), $U_{sw} = 5500$ Hz is shown for an operating point with nominal speed and load. The solution of Equation (4) is indicated with a times mark (×) corresponding to $\lambda_{xy} = 1$, $\lambda_{sw} = 92 \times 10^{-5}$. It can be seen that the optimal solution is close to the edge of the feasible region as it usually happens in constrained optimization problems. Another example is

presented in Figure 3(right) where the operating point is characterized by low speed and load (about 30% of nominal value). Please note that the low speed zone is challenging due to the apparition of large $x-y$ currents [24]. In this case, the solution of Equation (4) takes place for $\lambda_{xy} = 1.64$, $\lambda_{sw} = 51 \times 10^{-5}$. It can be seen that the optimal parameters are quite different for the two operating points considered, even if the admissible limits U are not changed.

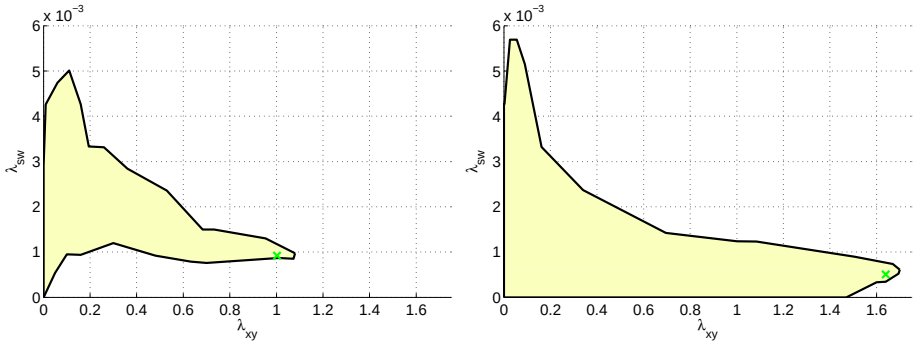

Figure 3. Examples of feasible regions for nominal speed and load (**left**) and for low speed and load (**right**). The optimal solution is shown as a $\times$ mark on each region.

The same procedure is repeated for a partition of the operating space, producing an optimal value for the λ parameters that characterizes the optimal controller for each cell. In Table 2, the results are shown for a partition of moderate size (3×3). Please note that, for finer partitions, better results can be expected at the cost of more experimentation needed to obtain the local parameters. The acceptable limits are set as in the previous case as $U_{\alpha\beta} = 0.035$ (A), $U_{sw} = 5500$ Hz. The rows and columns in Table 2 are the indices (h, j) that define the cell as $[h\Delta\omega,\ (h+1)\Delta\omega] \times [j\Delta T,\ (j+1)\Delta T]$ with $\Delta\omega = 330$ (rmp) and $\Delta T = 1$ (A). The values inside each cell are the pair $\theta = (\lambda_{xy},\ \lambda_{sw})$. It can be seen that the optimal values of λ_{xy} lie in the interval $[0.15,\ 1.64]$ meaning that the higher value is an order of magnitude larger than the lower. Similarly, for λ_{sw}, the interval is $[11,\ 120] \times 10^{-5}$. In addition, a nonlinear and not obvious relationship between both parameters is appreciable.

Table 2. Optimal θ parameters for $U_{\alpha\beta} = 0.035$ (A), $U_{sw} = 5500$ (Hz).

	1	**2**	**3**
1	$(1.64,\ 51 \times 10^{-5})$	$(1.21,\ 56 \times 10^{-5})$	$(1.31,\ 68 \times 10^{-5})$
2	$(1.44,\ 11 \times 10^{-5})$	$(1.00,\ 92 \times 10^{-5})$	$(0.68,\ 120 \times 10^{-5})$
3	$(1.19,\ 16 \times 10^{-5})$	$(0.17,\ 86 \times 10^{-5})$	$(0.15,\ 24 \times 10^{-5})$

Controller Assessment

To assess the proposed scheduled PCC, a comparison with the traditional PCC is made. Several points covering the whole operating space have been considered. For each operating point, the constraints satisfaction is tested by checking the inequalities $E_{\alpha\beta} < U_{\alpha\beta}$ and $\max f_{sw} < U_{sw}$. The results are presented with the help of the graph in Figure 4, where red color is used to indicate constraint violation and green for constraint satisfaction. The left graph (Case A) is for $\lambda_{xy} = 0.5$, $\lambda_{sw} = 0$ which is used in a variety of publications [6,23]. The graph on the right (Case B) is obtained for $\lambda_{xy} = 0.14$, $\lambda_{sw} = 60 \times 10^{-5}$. For the proposed strategy of scheduled local parameters, all points satisfy the constraints and thus no graph is needed.

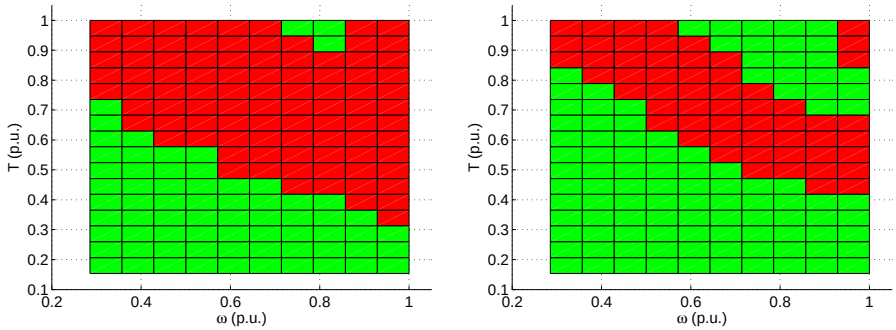

Figure 4. Constraint satisfaction of two PCC with fixed parameters: Case A for $\lambda_{xy} = 0.5$, $\lambda_{sw} = 0$ (**left**) and Case B for $\lambda_{xy} = 0.1$, $\lambda_{sw} = 60 \times 10^{-5}$ (**right**).

The minimization of E_{xy} is now checked. Figure 5 shows the histograms of E_{xy} for the two fixed controllers (Cases A and B above) and for the proposed scheduled PCC using for each operating point the value of θ indicated in Table 2. Please note that in the histogram all points are considered and not just on the green zone (where constraints are satisfied). It can be seen that the proposed controller provides the most adequate distribution of E_{xy} values, being placed at the lower end of the range. This comes in addition to meeting the constraints for all operating points, as already discussed. It is also interesting to note that Case A is better than Case B in terms of E_{xy} but its region of constraint satisfaction is more limited than that of Case B, as previously shown.

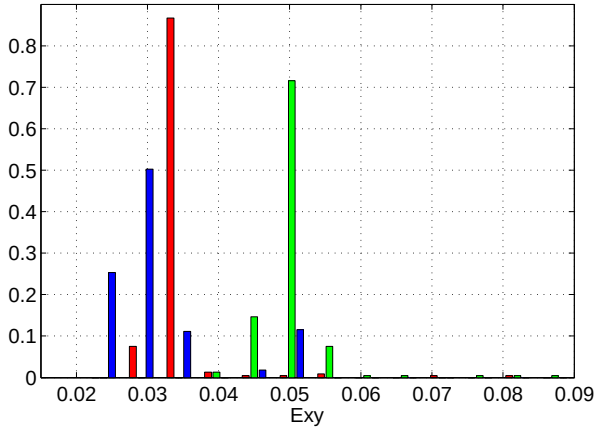

Figure 5. Histograms of E_{xy} for two traditional PCC: Case A (**red**) and Case B (**green**) and for the proposed scheduled PCC (**blue**).

An experimental comparison of the proposed locally tuned controller with a traditional PCC with fixed weighting factors is now presented. Figure 6 shows the trajectories of stator currents in α and x axes (similar results are logically obtained for β and y axes), along with the reference for α currents (for x currents the reference is zero as $x - y$ subspace generates only losses). Two operation points are considered: top row is for nominal speed and low load (Case A) and bottom row for nominal speed and 50% external torque (Case B). The tuning has been performed in this case to achieve tracking error below $U_{\alpha\beta} = 0.18$ (A) and a low commutation rate below $U_{sw} = 4$ kHz. The tuning for the fixed weights PCC is found to be $\lambda_{xy} = 0.5$, $\lambda_{sw} = 1200 \times 10^{-5}$. The locally tuned controller uses $\lambda_{xy} = 0.8$, $\lambda_{sw} = 1000 \times 10^{-5}$ for Operating Point A and $\lambda_{xy} = 0.5$, $\lambda_{sw} = 800 \times 10^{-5}$ for Operating Point B. From the results shown in Figure 6, it is clear that the extra degrees of freedom offered by the local tuning is exploited to obtain better tracking and less $x - y$ content without violating the constraints.

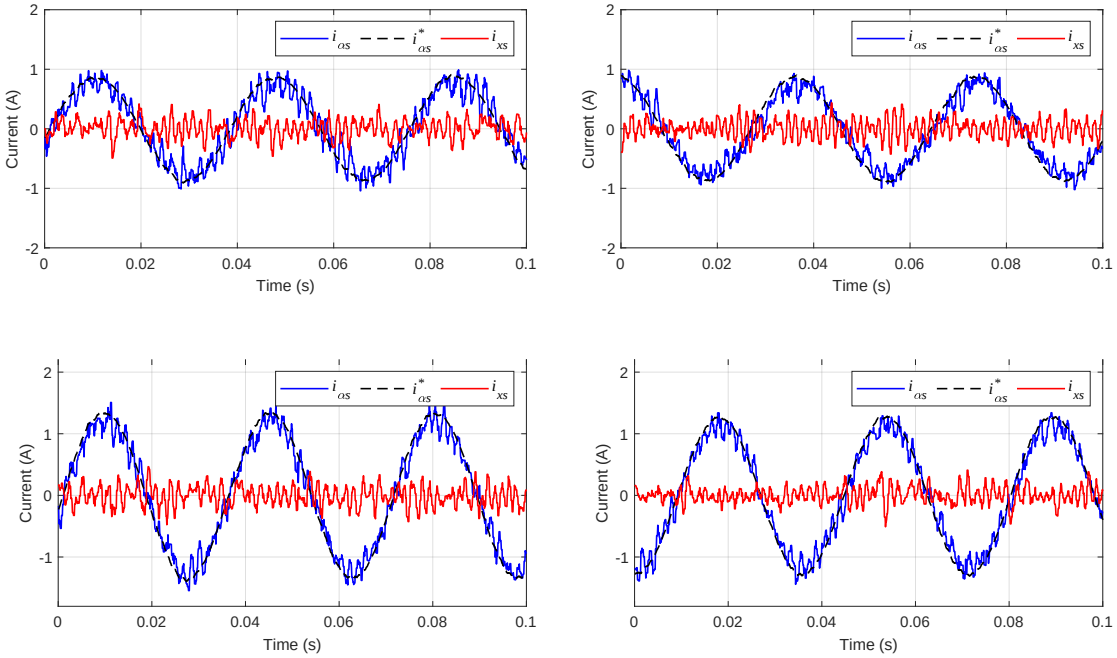

Figure 6. Experimental comparison of the proposed controller (**right**) against a traditional PCC using fixed weighting factors (**left**) at two operating regimes (**top** and **bottom** rows).

5. Conclusions

It has been shown how a modified tuning procedure, mathematically represented by an optimization problem, can solve the constraint handling problem of predictive stator current control for IM thanks to the use of locally tuned controllers. From the experiments, it can be concluded that the constraint feasibility problem has, in general, no solution for standard predictive control. The proposed scheme provides a means of obtaining good tracking performance without violating constraints in switching frequency and at the same time reducing parasitic currents of $x - y$ subspaces.

Author Contributions: Conceptualization, A.K.G. and M.R.A.; methodology, F.B. and M.R.A.; software, A.K.G. and C.M.; validation, A.K.G. and C.M.; formal analysis, A.K.G., M.R.A. and C.M.; investigation, A.K.; resources, F.B.; data curation, A.K.G.; writing—original draft preparation, A.K.G. and M.R.A.; writing—review and editing, A.K., M.R.A. and F.B.; visualization, F.B.; supervision, F.B. and M.R.A.; project administration, A.K. and C.M.; and funding acquisition, M.R.A.

Funding: This research was funded by Ministerio de Ciencia, Innovación y Universidades of Spain grant number RTI2018-101897-B-I00.

Conflicts of Interest: The authors declare no conflict of interest.

References

1. Holmes, D.; Martin, D. Implementation of a direct digital predictive current controller for single and three phase voltage source inverters. In Proceedings of the IAS '96. Conference Record of the 1996 IEEE Industry Applications Conference Thirty-First IAS Annual Meeting, San Diego, CA, USA, 6–10 October 1996; IEEE: Piscataway, NJ, USA, 1996; Volume 2, pp. 906–913.
2. Martin, C.; Barrero, F.; Arahal, M.R.; Duran, M.J. Model-Based Predictive Current Controllers in Multiphase Drives Dealing with Natural Reduction of Harmonic Distortion. *Energies* **2019**, *12*, 1679. [CrossRef]
3. Liu, C.; Luo, Y. Overview of advanced control strategies for electric machines. *Chin. J. Electr. Eng.* **2017**, *3*, 53–61.

4. Tenconi, A.; Rubino, S.; Bojoi, R. Model Predictive Control for Multiphase Motor Drives—A Technology Status Review. In Proceedings of the 2018 International Power Electronics Conference (IPEC-Niigata 2018-ECCE Asia), Niigata, Japan, 20–24 May 2018; IEEE: Piscataway, NJ, USA, 2018; pp. 732–739.
5. Camacho, E.F.; Bordons, C. *Model Predictive Control*; Springer: Berlin/Heidelberg, Germany, 2013.
6. Lim, C.S.; Levi, E.; Jones, M.; Rahim, N.; Hew, W.P. A Comparative Study of Synchronous Current Control Schemes Based on FCS-MPC and PI-PWM for a Two-Motor Three-Phase Drive. *IEEE Trans. Ind. Electron.* **2014**, *61*, 3867–3878. [CrossRef]
7. Arahal, M.R.; Barrero, F.; Durán, M.J.; Ortega, M.G.; Martín, C. Trade-offs analysis in predictive current control of multi-phase induction machines. *Control Eng. Pract.* **2018**, *81*, 105–113. [CrossRef]
8. Mamdouh, M.; Abido, M.; Hamouz, Z. Weighting Factor Selection Techniques for Predictive Torque Control of Induction Motor Drives: A Comparison Study. *Arab. J. Sci. Eng.* **2018**, *43*, 433–445. [CrossRef]
9. Hannan, M.; Ali, J.A.; Mohamed, A.; Hussain, A. Optimization techniques to enhance the performance of induction motor drives: A review. *Renew. Sustain. Energy Rev.* **2018**, *81*, 1611–1626. [CrossRef]
10. Arahal, M.R.; Kowal, A.; Barrero, F.; Castilla, M. Cost Function Optimization for Multi-phase Induction Machines Predictive Control. *Rev. Iberoam. Autom. Inf. Ind.* **2019**, *16*, 48–55. [CrossRef]
11. Khan, H.S.; Aamir, M.; Ali, M.; Waqar, A.; Ali, S.U.; Imtiaz, J. Finite Control Set Model Predictive Control for Parallel Connected Online UPS System under Unbalanced and Nonlinear Loads. *Energies* **2019**, *12*, 581. [CrossRef]
12. Abbaszadeh, A.; Khaburi, D.A.; Kennel, R.; Rodríguez, J. Hybrid exploration state for the simplified finite control set-model predictive control with a deadbeat solution for reducing the current ripple in permanent magnet synchronous motor. *IET Electr. Power Appl.* **2017**, *11*, 823–835. [CrossRef]
13. Vali, M.; Petrovic, V.; Boersma, S.; van Wingerden, J.W.; Pao, L.Y.; Kuhn, M. Adjoint-based model predictive control for optimal energy extraction in waked wind farms. *Control Eng. Pract.* **2019**, *84*, 48–62. [CrossRef]
14. Duran, M.J.; Levi, E.; Barrero, F. Multiphase Electric Drives: Introduction. In *Wiley Encyclopedia of Electrical and Electronics Engineering*; Wiley Online Library: Hoboken, NJ, USA, 2017; pp. 1–26.
15. Kali, Y.; Ayala, M.; Rodas, J.; Saad, M.; Doval-Gandoy, J.; Gregor, R.; Benjelloun, K. Current Control of a Six-Phase Induction Machine Drive Based on Discrete-Time Sliding Mode with Time Delay Estimation. *Energies* **2019**, *12*, 170. [CrossRef]
16. Martín, C.; Arahal, M.R.; Barrero, F.; Durán, M.J. Five-phase induction motor rotor current observer for finite control set model predictive control of stator current. *IEEE Trans. Ind. Electron.* **2016**, *63*, 4527–4538. [CrossRef]
17. Yaramasu, V.; Wu, B. *Model Predictive Control of Wind Energy Conversion Systems*; John Wiley & Sons: Hoboken, NJ, USA, 2016.
18. Rodas, J.; Barrero, F.; Arahal, M.R.; Martín, C.; Gregor, R. Online estimation of rotor variables in predictive current controllers: A case study using five-phase induction machines. *IEEE Trans. Ind. Electron.* **2016**, *63*, 5348–5356. [CrossRef]
19. Gonzalez-Prieto, I.; Duran, M.J.; Aciego, J.J.; Martin, C.; Barrero, F. Model predictive control of six-phase induction motor drives using virtual voltage vectors. *IEEE Trans. Ind. Electron.* **2018**, *65*, 27–37. [CrossRef]
20. Åström, K.J.; Wittenmark, B. On self tuning regulators. *Automatica* **1973**, *9*, 185–199. [CrossRef]
21. Desoer, C. Slowly varying system x = A (t) x. *IEEE Trans. Autom. Control* **1969**, *14*, 780–781. [CrossRef]
22. Hunt, K.J.; Johansen, T.A. Design and analysis of gain-scheduled control using local controller networks. *Int. J. Control* **1997**, *66*, 619–652. [CrossRef]
23. Martín, C.; Bermúdez, M.; Barrero, F.; Arahal, M.R.; Kestelyn, X.; Durán, M.J. Sensitivity of predictive controllers to parameter variation in five-phase induction motor drives. *Control Eng. Pract.* **2017**, *68*, 23–31. [CrossRef]
24. Echeikh, H.; Trabelsi, R.; Iqbal, A.; Bianchi, N.; Mimouni, M.F. Non-linear backstepping control of five-phase IM drive at low speed conditions—Experimental implementation. *ISA Trans.* **2016**, *65*, 244–253. [CrossRef] [PubMed]